ACS Biomaterials SCIENCE & ENGINEERING

pubs.acs.org/journal/abseba

Article

Prolonged Codelivery of Hemagglutinin and a TLR7/8 Agonist in a Supramolecular Polymer−Nanoparticle Hydrogel Enhances Potency and Breadth of Influenza Vaccination

Gillie A. Roth,[○] Olivia M. Saouaf,[○] Anton A. A. Smith, Emily C. Gale, Marcela Alcántara Hernández, Juliana Idoyaga, and Eric A. Appel*

Cite This: *ACS Biomater. Sci. Eng.* 2021, 7, 1889−1899

Read Online

ACCESS | Metrics & More | Article Recommendations | Supporting Information

ABSTRACT: The sustained release of vaccine cargo has been shown to improve humoral immune responses to challenging pathogens such as influenza. Extended codelivery of antigen and adjuvant prolongs germinal center reactions, thus improving antibody affinity maturation and the ability to neutralize the target pathogen. Here, we develop an injectable, physically cross-linked polymer−nanoparticle (PNP) hydrogel system to prolong the local codelivery of hemagglutinin and a toll-like receptor 7/8 agonist (TLR7/8a) adjuvant. By tethering the TLR7/8a to a NP motif within the hydrogels (TLR7/8a-NP), the dynamic mesh of the PNP hydrogels enables codiffusion of the adjuvant and protein antigen (hemagglutinin), therefore enabling sustained codelivery of these two physicochemically distinct molecules. We show that subcutaneous delivery of PNP hydrogels carrying hemagglutinin and TLR7/8a-NP in mice improves the magnitude and duration of antibody titers in response to a single injection vaccination compared to clinically used adjuvants. Furthermore, the PNP gel-based slow delivery of influenza vaccines led to increased breadth of antibody responses against future influenza variants, including a future pandemic variant, compared to clinical adjuvants. In summary, this work introduces a simple and effective vaccine delivery platform that increases the potency and durability of influenza subunit vaccines.

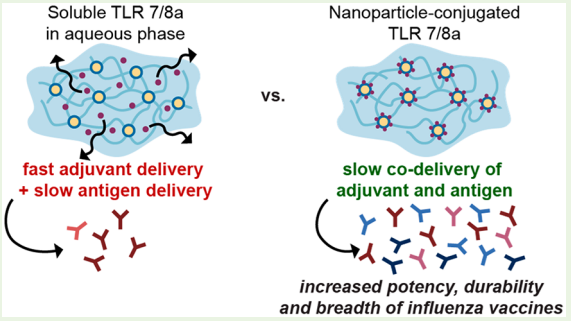

KEYWORDS: *immunoengineering, biomaterials, hydrogels, vaccines, drug delivery*

INTRODUCTION

Seasonal influenza causes roughly 500,000 deaths annually worldwide, and every "bad" flu year reminds us that current flu vaccine technologies are outdated and inadequate. A virulent pandemic such as the Spanish flu outbreak of 1918, which killed over 40 million people worldwide, could kill hundreds of millions today from more rapid transmission fueled by crowded cities and active global transportation.[1] Indeed, new influenza strains with the potential to become pandemics continue to arise worldwide, including a recently described swine influenza variant that comprises genetic mutations from European and Asian birds.[2] An efficacious vaccine would elicit a persistent antibody response and high-affinity broadly neutralizing antibodies (bnAbs) against the structurally diverse and rapidly mutating hemagglutinin (HA) viral envelope glycoprotein.[3,4] BnAbs are characterized by extensive somatic hypermutation (SHM) occurring during affinity maturation in germinal centers (GCs) within lymphoid organs.[5,6] Yet, vaccines promoting long-lived GCs and prolonging the SHM process to generate high affinity bnAbs remain elusive.[7−10] Three parameters are crucial to enhancing affinity maturation: (i) sustained vaccine exposure to prolong affinity maturation, (ii) the use of adjuvants such as toll-like receptor agonists (TLRa), and (iii) precise codelivery of the subunit vaccine components.[9,11] While reports indicate that subunit vaccines comprising multiple TLRa molecules elicit better immune memory and stronger antibody responses,[12−14] controlled encapsulation and release of physicochemically distinct reagents has historically been challenging or impossible.[13,15,16] Furthermore, adjuvants alone typically do not provide sufficient immunological driving forces for promoting extensive affinity maturation, and reports indicate that prolonged vaccine exposure can have a profound effect on the magnitude and quality of the immune response.[17−24] Yet, there are few delivery platforms reported to date that are able to achieve controlled codelivery of physicochemically distinct antigens and TLRa molecules over prolonged time frames.[20,25] To

Special Issue: Nanomedicine Advances in Infectious Diseases

Received: October 17, 2020
Accepted: December 23, 2020
Published: January 6, 2021

address this challenge, we have developed a controlled release technology for prolonged codelivery of an influenza subunit vaccine comprising hemagglutinin and small molecule imidazoquinoline TLR7/8a, which has been shown to be a potent driver of an efficacious influenza vaccine response.[13]

A common challenge when delivering small molecule adjuvants is their tendency to diffuse directly into circulation, often causing systemic toxicity instead of targeted immune modulation in lymph tissues.[26] A popular solution for augmenting the pharmacokinetics and biodistribution of small molecule adjuvants, especially those which are fairly hydrophilic (i.e., logP < 2), is conjugation to nanoparticles which increases the size compared to soluble adjuvants. This increase in size improves passive diffusion to the lymph nodes (LN), thereby decreasing systemic exposure and associated toxicities.[27] Furthermore, these nanoparticle formulations are able to prolong the stability and enhance the potency of the adjuvants.[28] Nanoparticle conjugation or encapsulation of adjuvants has been shown to improve the activation of antigen presenting cells (APCs) such as macrophages and dendritic cells since nanoparticle sizes can be tuned for optimal endocytosis.[13,26,29] Though nanoparticle conjugation is beneficial for improving the ability of adjuvant molecules to reach the target cells, they do not provide a solution for sustained retention of the adjuvant for a more prolonged inflammatory response.

Injectable hydrogels and depot technologies provide an avenue for achieving sustained release of vaccine cargo with minimally invasive administration (i.e., through direct injection).[30−35] In previous work, we showed that polymer−nanoparticle (PNP) hydrogels can be used as a prolonged delivery platform for vaccine administration to enhance the magnitude and duration of GC responses, improving the durability of antibody responses and enhancing antibody affinity maturation.[19] PNP hydrogels are held together by dynamic, multivalent noncovalent interactions between two structural motifs, which include a cellulosic biopolymer and a nanoparticle (NP), allowing for them to be easily injected through standard needles while also creating a robust depot at their injection site.[20,36−41] The simplicity and scalability of the fabrication process allows for facile manufacturing, which is a necessary design constraint for future translation.[42−44] These hydrogels are highly modular and can be adapted to deliver a wide range of cargo. When the cargo is sufficiently large, its diffusion will be restricted by the network of the hydrogel and will diffuse at the same rate as the dynamic rearrangement of the gel's polymer network itself.[35,38,45]

The unique cargo delivery features of the PNP hydrogels allow for creating dependable sustained codelivery of multicomponent vaccine formulations comprising large cargo (e.g., those with a hydrodynamic radius above ∼3 nm). Yet, when a molecule is smaller than the polymer mesh (e.g., small molecule imidazoquinoline TLR7/8a molecules), it is able to diffuse relatively unhindered by the polymer network. In this work, we sought to engineer an approach to PNP hydrogel formulation to create a platform for sustained codelivery of encapsulated antigens with a potent and highly specific TLR7/8a molecule through conjugation of the TLR7/8a to the NP structural motif within the PNP hydrogel network. We show that the TLR7/8a activity is not affected by the conjugation to the NP construct and PNP hydrogel mechanical properties are unperturbed when formulated with TLR7/8a-conjugated NPs rather than standard NPs. We confirm that NP-tethered TLR7/8a and a well-studied influenza antigen hemagglutinin (HA) diffuse at similar rates within these materials, allowing for sustained codelivery. Furthermore, we demonstrate that sustained delivery of this influenza vaccine leads to an antibody response with enhanced potency, durability, and breadth compared to clinical adjuvant systems. Overall, this study demonstrates the potential of the injectable PNP hydrogel platform to be adapted toward sustained codelivery of diverse adjuvants and antigens of interest to enhance humoral immune responses.

MATERIALS AND METHODS

Materials. HPMC (meets USP testing specifications), *N*,*N*-diisopropylethylamine (Hunig's base), diethyl ether, hexanes, *N*-methyl-2-pyrrolidone (NMP), lactide (LA), dichloromethane (DCM), diazobicylcoundecene (DBU), and 1-dodecylisocynate were purchased from Sigma-Aldrich and used as received. Monomethoxy-PEG (5 kDa) purchased from Sigma-Aldrich was purified by azeotropic distillation with toluene prior to use. AF647-DBCO was purchased from Thermo Fisher and used as received. HIS-Lite-Cy3 Bis NTA-Ni complex was purchased from AAT Bioquest and used as received.

Polymer Characterization. Once polymer synthesis was completed, ^{1}H nuclear magnetic resonance (NMR) was performed to determine number-average molecular weight (Mn) using an Inova 300. All samples were dissolved in d-chloroform for characterization. Samples were passed through two size exclusion chromatography columns (Resolve Mixed Bed Low DVB, ID 7.8 mm, Mw range 200−600 000 g/mol, Jordi Laboratories) in a mobile phase of *N*,*N*-dimethylformamide (DMF) with 0.1 M LiBr at 35 °C and a flow rate of 1.0 mL/min (Dionex Ultimate 3000 pump, degasser, and autosampler (Thermo Fisher Scientific)), and subsequently the ASTRA software package (Wyatt Technology Corporation) was used to obtain absolute molecular weight and polydispersity. A HELEOS II light scattering detector (Wyatt Technology Corporation) operating at 659 nm and an Optilab T-rEX (Wyatt Technology Corporation) refractive index detector operating at 658 nm were used for detection. Dn/dc values for PEG and PLA, 0.0442 and 0.019, respectively, in the mobile phase, were calculated using

$$(dn/dc)_{ab} = (dn/dc)_a(wt\%)_a + (dn/dc)_b(wt\%)_b \quad (1)$$

after having determined the dn/dc values for PEG and PEG-PLA polymers of known weight fractions (via ^{1}H NMR spectroscopy) in the ASTRA software package by batch injection of 3 samples of known concentrations into an Optilab T-rEX refractive index detector.

Preparation of HPMC-C_{12}. HPMC-C_{12} was prepared according to previously reported procedures.[37] HPMC (1.0 g) was stirred at 80 °C for 1 h until dissolved in NMP (40 mL) before removing from heat. In a separate vessel, Hunig's base (catalyst, ∼3 drops) and 1-dodecylisocynate (105 mg, 0.5 mmol) were dissolved in NMP (5.0 mL). Once the HPMC solution mixture had cooled to room temperature, the catalyst solution was added dropwise, and this mixture was then stirred at room temperature for 16 h. This solution was then poured into acetone for precipitation. The precipitate was decanted, redissolved in water (∼2 wt %), and dialyzed in dialysis tubing for 3−4 days. The polymer was cryodesiccated and reconstituted to 60 mg/mL in sterile PBS.

Preparation of PEG-PLA. PEG-PLA was prepared as previously reported.[37] Monomethoxy-PEG (5 kDa; 0.25 g, 4.1 mmol) and DBU (15 μL, 0.1 mmol; 1.4 mol % relative to LA) were dissolved in anhydrous dichloromethane (1.0 mL). LA (1.0 g, 6.9 mmol) in anhydrous DCM (3.0 mL) was mildly heated for dissolution. The LA solution was added rapidly to the PEG/DBU solution and stirred for 10 min. This reaction mixture was quenched and precipitated by addition to a 1:1 hexane and ethyl ether solution. The synthesized PEG-PLA precipitate was collected and dried under vacuum. Gel permeation chromatography (GPC) was used to verify that the

https://dx.doi.org/10.1021/acsbiomaterials.0c01496
ACS Biomater. Sci. Eng. 2021, 7, 1889−1899

molecular weight and dispersity of polymers met our quality control (QC) parameters.

Preparation of TLR7/8a-PEG-PLA. TLR7/8a-PEG-PLA was prepared according to a literature report,[29] and the protocols will be briefly described here. Azide-PEG-PLA was prepared using N_3-PEG-OH (0.5 g, 5 kDa, 100 μmol) in anhydrous DCM (2.0 mL) with DBU (30 μL, 30 mg, 0.20 mmol) which was added quickly to a stirring solution of LA (2.0 g, 13.9 mmol) in anhydrous DCM (6.0 mL). The solution was stirred for 10 min, after which 2 drops of acetic acid was added to quench the reaction, and the polymer was precipitated into a 1:1 mixture of hexanes and diethyl ether. The polymer was redissolved in a minimal amount of acetone and precipitated again in diethyl ether and dried in vacuo. GPC was used to verify that the molecular weight and dispersity of polymers meet our QC parameters.

A 20 mL scintillation vial was charged with the TLR 7/8 agonist alkyne (14 mg, 30 μmol), and azido poly(ethylene oxide)-*b*-poly(D,L-lactide) ($PEG_{5\ kDa}$-$PLA_{20\ kDa}$, 0.5 g, 20 μmol) was dissolved in NMP (4.0 mL) and flushed with nitrogen for 10 min. Next, a degassed solution (0.1 mL) of CuBr (3.7 mg/mL) and THPTA (16 mg/mL) was added. This reaction mixture was then further flushed with nitrogen gas for 10 min. The reaction mixture was stirred for 16 h at room temperature and added to diethyl ether in a 50 mL centrifuge tube for precipitation to recover the polymer. The polymer was next dissolved in ethyl acetate and precipitated into diethyl ether, followed by collection and drying in vacuo. GPC was used to verify that the molecular weight was not altered by conjugation. Conjugation was confirmed by ^{1}H NMR spectroscopy and increased UV absorption as indicated by GPC (DMF) eluagram.

General Preparation of PEG-PLA NPs, TLR7/8a-NPs, and AF647-NPs. NPs were prepared as previously reported.[37,46] A 1 mL solution of PEG-PLA in DMSO (50 mg/mL) was added in a dropwise fashion to 10 mL of water at room temperature stirred at 600 rpm. NPs were characterized by dynamic light scattering (DLS) to find the NP diameter and zeta potential (PEG-PLA NPs, 31 ± 3 nm, −28 ± 7 mV; TLR7/8a-PEG-PLA NPs, 31 ± 3 nm, −10 ± 7 mV) (SI Table 1). AF647 NPs were prepared using a combination of PEG-PLA (25 mg) and unconjugated azide-PEG-PLA (25 mg) and then functionalized following purification by mixing azide-functional NPs (500 μL, 20 wt %) with AF647-DBCO (5 μL, 1 mg/mL).

General PNP Hydrogel Preparation. The PNP hydrogel formulation contained 2 wt % HPMC-C_{12} and 10 wt % PEG-PLA NPs in PBS. These gels were made by mixing a 2:3:1 weight ratio of 6 wt % HPMC-C_{12} polymer solution, 20 wt % NP solution, and PBS. For TLR7/8a-NP gels, the PEG-PLA NPs were made up of a mixture of TLR7/8a conjugated NP and nonconjugated NP based on the desired dose of adjuvant. The solutions were mixed with an elbow mixer and loaded into a syringe.

Vaccine Formulations. The influenza vaccine contained a 2 μg dose of Influenza A H1N1 (A/Brisbane/59/2007) hemagglutinin (HA)(Sino Biological) and an approximate TLR 7/8 agonist dose of 50 μg. For the PNP hydrogels, the vaccine cargo was added at the appropriate concentration into the PBS component of the gel before adding the polymer and NP solutions, as described above. For AddaVax (InvivoGen; squalene based oil-in-water nanoemulsion similar to MF59, which is a proprietary adjuvant produced by Novartis) and Alhydrogel (Alum; InvivoGen) vaccines, the formulations were prepared according to the manufacturer's instructions with a 2 μg dose of HA.

***In Vitro* RAW-Blue Reporter Assay.** The RAW-Blue reporter cell line (InvivoGen, raw-sp) was used to measure TLR7/8 agonist activity. Cells were cultured at 37 °C with 5% CO_2 in Dulbecco's modified Eagle's medium (DMEM; Thermo Fisher Scientific) supplemented with D-glucose (4.5 g/L), L-glutamine (2 mM), penicillin (100 U/mL)/streptomycin (100 μg), zeocin (100 μg/mL; Invi-vogen), and 10% heat inactivated fetal bovine serum (Atlanta Biologicals). Soluble TLR7/8a (R848) or TLR7/8a-NPs (20 μL) at a final concentration of 5 μg/mL was added to a 96-well tissue culture treated plate. Approximately 100,000 cells in 180 μL of media were added to each well. Cells were cultured for 20 h at 37 °C in a CO_2 incubator before following manufacturer instructions for SEAP quantification (absorbance at 655 nm).

Gel Rheological Characterization. Rheological characterization was conducted with a TA Instruments Discovery HR-2 torque-controlled rheometer fitted with a Peltier stage. All measurements were performed using a serrated 20 mm plate geometry at 25 °C. Dynamic oscillatory frequency sweep measurements were performed with a constant torque (2 μN·m; σ = 1.27 Pa) from 0.1 rad/s to 100 rad/s. Steady shear experiments were performed from 0.1 to 100 s^{-1}. Yield stress values were found using stress ramp experiments.

FRAP Analysis. Hydrogels were made as stated above, each with a unique fluorescent component: (i) free fluorescein, (ii) AF647-NP, (iii) rhodamine-conjugated HPMC-C_{12}, or (iv) His-tagged hemagglutinin conjugated with HIS-Lite-Cy3 Bis NTA-Ni complex. Gels were placed onto glass slides and imaged using a confocal LSM780 microscope. Samples were imaged using low intensity lasers to collect an initial level of fluorescence. Then a high intensity laser was focused on a region of interest (ROI) with a 25 μm diameter for 10 s in order to bleach a circular area. Fluorescence data was then recorded for 4 min to create an exponential fluorescence recovery curve. Samples were taken from different regions of each gel (n = 2−5) The diffusion coefficient was calculated as[47]

$$D = \gamma_D(\omega^2/4\tau_{1/2}) \quad (2)$$

where the constant $\gamma_D = \tau_{1/2}/\tau_D$, with $\tau_{1/2}$ being the half-time of the recovery, τ_D the characteristic diffusion time, both yielded by the ZEN software, and ω the radius of the bleached ROI (12.5 μm).

Animal Protocol. All animal procedures were performed in accordance with National Institutes of Health guidelines, with the approval of Stanford Administrative Panel on Laboratory Animal Care.

Mice and Vaccination. C57BL/6 (B6) mice purchased from Charles River were used for study of immune response and housed at Stanford University. Female mice from 6 to 10 weeks of age at the beginning of the experiment were used. The mice were shaved several days before vaccine administration and received a subcutaneous injection (100 μL administration volume) of gel or bolus vaccine on their backs under brief isoflurane anesthesia. Mouse blood was collected via tail vein bleeds for survival studies or through cardiac puncture for terminal studies.

Antibody Concentration. Serum IgG antibody titers for the influenza vaccine were measure using an ELISA. Ni-coated plates (Thermofisher) were coated with HA (Sino Biological) at 2.5 μg/mL in PBS for 1 h at 25 °C and blocked with PBS containing 1% BSA for 1 h at 25 °C. A standard curve was created by pooling serum and completing serial dilutions (2×) before adding to the plate, and serum samples were diluted 1:200 (Alum group) or 1:1,000 (Gel and AddaVax groups) and added to plates. After 2 h at °C, goat-anti-mouse IgG Fc-HRP (1:10,000, Invitrogen, A16084) was added for 1 h at 25 °C. Plates were developed with TMB substrate (TMB ELISA Substrate (High Sensitivity), Abcam). The reaction was stopped with 1 M HCl. The plates were analyzed with a Synergy H1 Microplate Reader (BioTek Instruments) at 450 nm. Serum antibody titers were calculated from a standard curve and represented as the dilution required to reach the detection limit.

Serum IgG1, IgG2b, and IgG2c antibody titers against A/Brisbane/59/2007 HA and IgG titers against A/California/07/2009, A/Michigan/45/2015, and A/Puerto Rico/8-WG/1934 HA were measure using an end point ELISA. Ni-coated plates (Thermofisher) were coated with HA (Sino Biological) at 2.5 μg/mL in PBS for 1 h at 25 °C and blocked with PBS containing 1% BSA for 1 h at 25 °C. First, serum was diluted 1:250 and then 4-fold serial dilutions were performed up to 1:4,096,000 dilution. Titrations were added to plates and after 2 h at 25 °C, HRP-conjugated goat-anti-mouse IgG1 (Abcam, ab97240), IgG2b (Chondrex, 3016), IgG2C (Abcam, ab97255), or IgG (Invitrogen, A16084) was added at a 1:10,000 dilution for 1 h at 25 °C. Plates were developed with TMB substrate (TMB ELISA Substrate (High Sensitivity), Abcam). The reaction was stopped with 1 M HCl. The plates were analyzed with a Synergy

https://dx.doi.org/10.1021/acsbiomaterials.0c01496
ACS Biomater. Sci. Eng. 2021, 7, 1889−1899

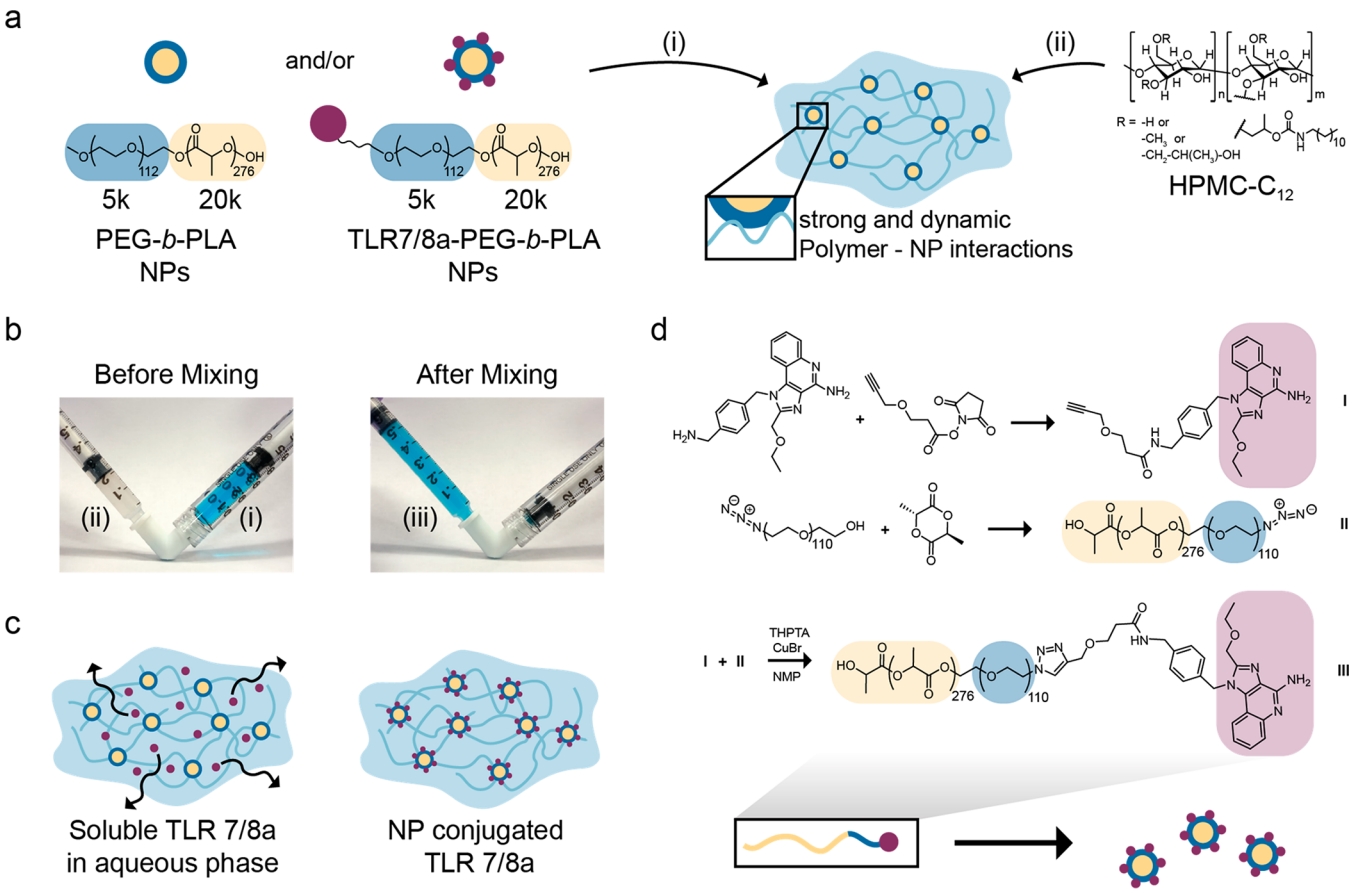

Figure 1. Fabrication of polymer−nanoparticle (PNP) hydrogels comprising TLR7/8a-functional nanoparticles. (a, b) PNP hydrogels are formed when (i) poly(ethylene glycol)-*b*-poly(lactic acid) (PEG-PLA) nanoparticles (NPs) or TLR7/8a-conjugated PEG-PLA NPs are combined with (ii) dodecyl-modified hydroxypropylmethylcellulose (HPMC-C_{12}). Multivalent and dynamic noncovalent interactions between the polymer and NPs constitute physical cross-links that form the hydrogel structure. Vaccine cargo can be added to the aqueous NP solution before mixing, which yields complete encapsulation into the fabricated hydrogels. (b) (iii) A homogeneous gel is easily achieved using an elbow mixer or a spatula. (c) To ensure small molecule cargo such as TLR7/8a achieves sustained delivery, it can be chemically conjugated to the PEG-PLA NP structural motif of the hydrogels. (d) NHS coupling of alykyne functionality to TLR7/8a (**I**) followed by copper-catalyzed "click" coupling to azide-terminated PEG-PLA (**II**) yields PEG-PLA with the TLR7/8a (purple) presenting on the hydrophilic PEG (blue) terminus of the block copolymer (**III**). This polymer is then nanoprecipitated into water to form TLR7/8a-functional NPs.

H1Microplate Reader (BioTek Instruments) at 450 nm. End point titers were defined as the reciprocal of the highest serum dilution that gave an optical density above 0.1.

Statistical Analysis. All statistical methods are indicated in the figure captions. Comparisons between two groups were conducted by a two-tailed Student's *t* test. A one-way ANOVA test with a Tukey's multiple comparisons test was used for comparison across multiple groups. Statistical analysis was run using GraphPad Prism 7.04 (GraphPad Software). Statistical significance was considered as $p < 0.05$.

RESULTS

In prior work, we have described the synthesis of injectable PNP hydrogel materials that are highly efficient in loading vaccine components for tunable codelivery of subunit vaccine components over prolonged time frames.[20] These PNP hydrogels form rapidly upon mixing of aqueous solutions of hydroxypropyl methylcellulose derivatives (HPMC-C_{12}) with biodegradable polymeric NPs composed of poly(ethylene glycol)-*b*-poly(lactic acid) (PEG-PLA) (Figure 1a).[46] Following mixing with an elbow mixer or a spatula, the two solutions form multivalent and dynamic noncovalent, multivalent interactions between the PEG-PLA NPs and the hydrophobically modified HPMC polymer which creates the physical cross-links that form to the hydrogel structure (Figure 1b). This facile synthesis allows the creation of hydrogel formulations with a range of mechanical properties by simply changing the ratio of HPMC-C_{12} to NP to an aqueous solution.[37] For this manuscript, we chose to use a 2 wt % HPMC-C_{12} + 10 wt % NP formulation due to the improved efficacy seen with this formulation in the delivery of OVA-based subunit vaccines.[20]

To apply this platform toward the influenza antigen hemagglutinin (HA), which is the most commonly used antigen in influenza subunit vaccines, we further adapted the hydrogel to ensure sustained codelivery of the subunit components. In these studies, we used a TLR7/8a adjuvant because TLR7/8a has been previously shown to elicit strong titers against HA and has demonstrated promise for clinical translation.[13] To ensure sustained coadministration of HA and the TLR7/8a, which is a small molecule (314 Da), we tethered the TLR 7/8a to the PEG-PLA NPs that form the PNP hydrogel network together with HPMC-C_{12} (Figure 1c,d). To synthesize the TLR7/8a conjugated PEG-PLA, alkyne modified TLR7/a was coupled to azide terminated PEG-PLA. NMR was used to confirm conjugation (SI Figure 1). To generate TLR7/8a-NPs, the TLR 7/8a conjugated PEG-PLA

https://dx.doi.org/10.1021/acsbiomaterials.0c01496
ACS Biomater. Sci. Eng. 2021, 7, 1889−1899

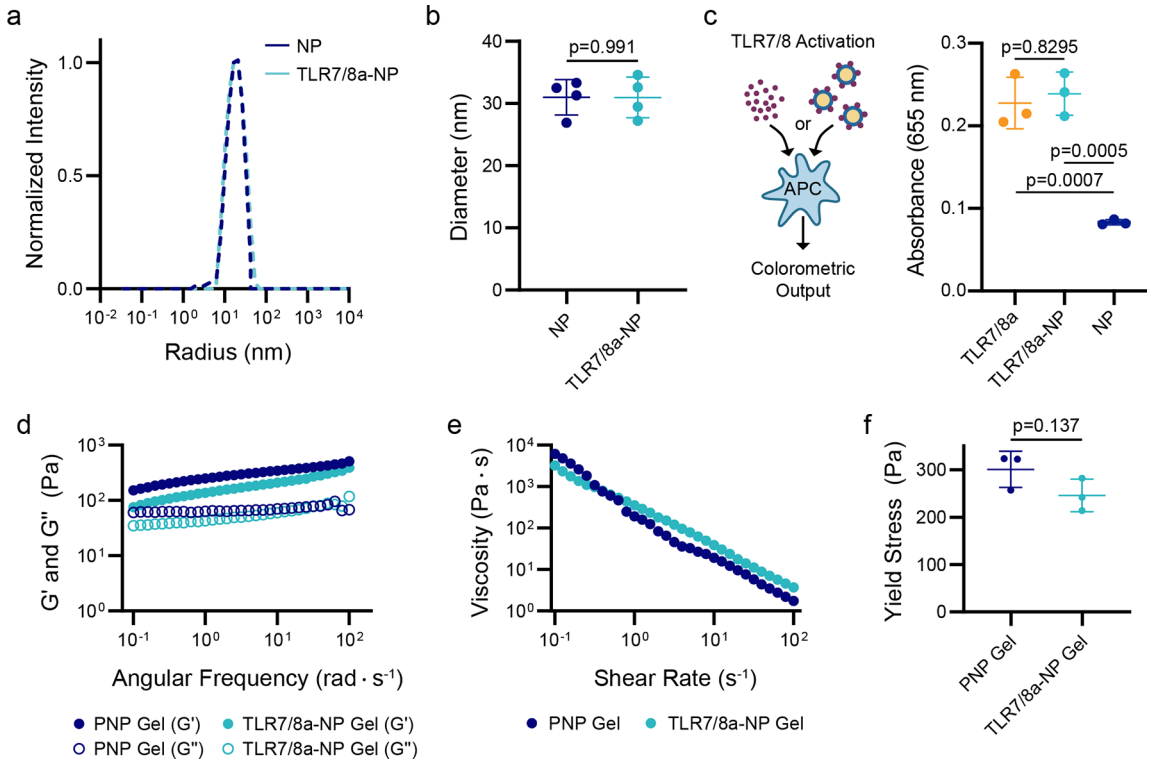

Figure 2. Nanoparticle and gel characterization. (a) Characteristic dynamic light scattering (DLS) curves for PEG-PLA NPs (teal) and TLR7/8a-NPs (dark blue). (b) Hydrodynamic diameters for PEG-PLA NPs and TLR7/8a-NPs for four independent experiments measured with DLS (n = 4). (c) Activation of RAW-Blue macrophage cells after a 20-h incubation with soluble TLR7/8a, TLR7/8a-NPs, or unconjugated NPs at 5 μg/well of the adjuvant. Activation was determined using QUANTI-Blue (n = 3). (d) Frequency-dependent (σ = 1.8 Pa, 25 °C) oscillatory shear rheology and (e) steady shear rheology of the PNP gel with PEG-PLA NPs (dark blue) or TLR7/8a-NPs (teal). (f) Yield stress values from stress ramp measurements (n = 3). All error bars are mean ± s.d. and P values were determined by a two-tailed t test (b, f) or one-way ANOVA with Tukey's post hoc test (c).

polymers were mixed in a 1:1 ratio with unconjugated PEG-PLA and nanoprecipitated into water.

It was important to confirm that the TLR7/8a conjugation did not affect the NP properties or the immunogenicity of the adjuvant, so the TLR7/8a-NP were characterized with multiple assays. The TLR7/8a-NP and plain NPs were characterized using dynamic light scattering (DLS) and were both found to have hydrodynamic diameters (D_H) of 31 ± 3 nm s.d. (Figure 2a, b, SI Table 1), showing that the adjuvant conjugation did not alter the NP diameter. To ensure that TLR7/8a-NPs were still able to activate innate immune cells, RAW-Blue macrophage cells were incubated for 20 h with either TLR7/8a-NP or soluble TLR7/8a (R848) and their NF-kB and AP-1 activation was measured. We saw similar levels of activation for soluble and conjugated TLR7/8a-NP with absorbance values of 0.23 and 0.24, respectively (Figure 2c), verified with a titrated range of adjuvant concentrations[28] (SI Figure 2). TLR7/8a activity depends on multiple factors, including cell uptake (which can be enhanced by nanoparticles), concentration, and potency (which can be affected by valency).[27] These assays demonstrated that we were able to synthesize stable TLR7/8a-NPs capable of potent TLR7/8 activation.

To ensure that the conjugation of TLR7/8a to the NPs did not influence the mechanical properties of the PNP hydrogels, rheological characterization comparing hydrogels formulated with TLR7/8a-NPs and standard PEG-PLA NPs was performed. Frequency-dependent oscillatory shear experiments, performed in the linear viscoelastic regime, demonstrated that TLR7/8a conjugation to the NP does not influence the PNP hydrogels' frequency-dependent rheology (Figure 2d). At a representative angular frequency (ω = 10 rad/s), the standard PNP gel and TLR7/8a-NP gel exhibited storage moduli (G') of 350 and 210 Pa, respectively. The angular frequency sweep rheological data also showed that both unadjuvanted and adjuvanted gels exhibited solid-like properties across the full range of frequencies tested, with the G' remaining above the loss modulus (G'') at all frequencies evaluated (Figure 2d). To compare the gels' abilities to shear-thin and behave similarly in injection conditions, a shear rate sweep was performed. The viscosity of both PNP hydrogels decreased around 3 orders of magnitude as shear rates increased and exhibited similar shear-rate dependent viscosities (Figure 2e). A stress ramp showed the yield stress of these materials to be approximately 300 and 250 Pa for the standard PNP gel and TLR7/8a-NP gels, respectively (Figure 2f). These yield stress values demonstrate each gels' ability to remain solid-like under low stresses (i.e., pre- and postinjection), thereby preserving a robust gel structure postinjection and inhibiting dissipation via flow from the injection site. This feature is critical for facilitating the creation of a local inflammatory niche.[20,48,49]

To characterize the diffusion rates of vaccine components within the gel, fluorescence recovery after photobleaching (FRAP) measurements was performed (Figure 3a). In these experiments, a fluorescent moiety was conjugated to NPs, HA, or HPMC-C_{12} and these components were formed into a gel (free fluorescein served as a proxy for the similarly sized small molecule cargo TLR7/8a). A defined circular region of the gel

https://dx.doi.org/10.1021/acsbiomaterials.0c01496
ACS Biomater. Sci. Eng. 2021, 7, 1889−1899

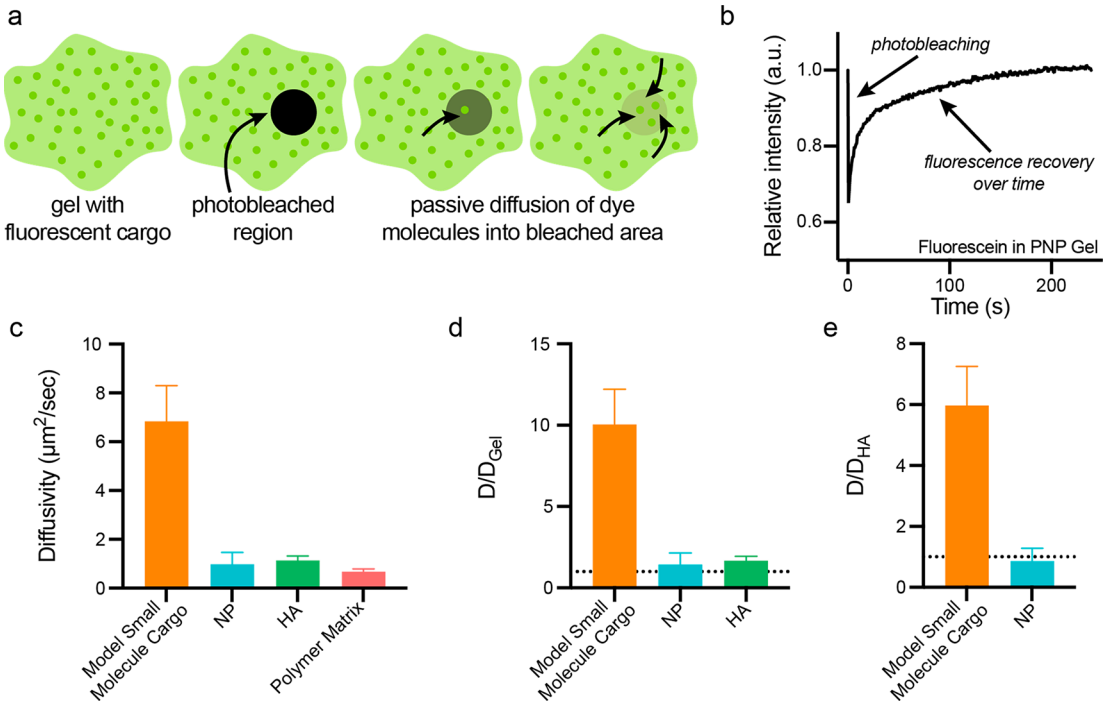

Figure 3. Diffusivity of vaccine and gel components. (a) FRAP measurements are taken of dye-conjugated components of the gel or entrapped dye-conjugated cargo by photobleaching a circular region and measuring the recovery of fluorescence as dye-conjugated species diffuse back into the photobleached region. (b) Representative graph of fluorescence recovery data for the small molecule fluorescein in a PNP gel. (c) Diffusivity calculated from FRAP measurements in a PNP gel (n = 2−5) for each fluorescently labeled gel component and vaccine component: model small molecule cargo (untethered fluorescein representing untethered TLR7/8a), NP (NP-tethered AF647 representing TLR7/8a-NP), HA (Cy3-labeled HA), and polymer matrix (rhodamine-conjugated HPMC-C_{12}). (d) Component diffusivities normalized by D_{gel} (the polymer matrix diffusivity) show NPs and HA are caught in the hydrogel network. Dotted line is at D/D_{gel} = 1. (e) Measured diffusivities demonstrate that molecules attached to NPs (NP) diffuse at a similar rate to HA, allowing for sustained codelivery, while untethered small molecule cargo quickly diffuses out of the gel. Dotted line is at D/D_{HA} = 1.

was bleached via exposure to intense light. Fluorescence recovery was measured as particles from outside the region diffused in, generating a curve from which the diffusivity of the gel components and entrapped cargo was calculated (Figure 3b). Small molecule cargo such as free fluorescein was shown to diffuse faster than any other component in the gel, indicating that untethered TLR7/8a is smaller than the gel's mesh size, diffusing rapidly out of the gel and thereby not capable of sustained codelivery with HA antigen (Figure 3c, SI Table 2). When compared to the diffusivity of the polymer matrix, measured as the diffusivity of HPMC-C_{12}, both NPs and HA had ratios close to 1, demonstrating that both HA and NP-tethered TLR7/8a are "caught" within the hydrogel mesh and diffuse with the network as intermolecular interactions break and reform (Figure 3d). Finally, a comparison of NP-tethered and untethered moieties to the diffusion of HA indicates that NP-tethered TLR7/8a achieves codelivery with the antigen as their ratio is close to 1, while untethered adjuvant diffuses much more quickly than the antigen (Figure 3e). Assuming a spherical 100 μL gel (the typical administration volume for our mouse studies, *vide infra*), Brownian motion approximates the time frame of HA (D = 1.1 ± 0.18 $\mu m^2/s$) and TLR7/8a-NP (D = 1.0 ± 0.48 $\mu m^2/s$) release from the gel to be 16 and 14.5 days, respectively, indicating that our delivery platform enables prolonged codelivery of antigen and adjuvant over the course of 2−3 weeks (SI-Cargo Release Time).

Next, to interrogate how sustained codelivery of antigen and adjuvant influences humoral immunity toward the HA antigen from A/Brisbane/59/2007 (H1N1), we quantified the HA-specific IgG antibody titers after single subcutaneous administration of HA in the TLR7/8a-NP gels compared with unconjugated TLR7/8a (R848) in a standard gel (TLR7/8a-Sol Gel). We also compared these formulations to delivering HA as a bolus with clinically relevant adjuvants AddaVax, which has a similar formulation to MF59, the most potent influenza vaccine adjuvant used clinically, and Alum, an aluminum hydroxide adjuvant which has been used previously in clinical influenza vaccine formulations[50,51] (Figure 4a,b). Subcutaneous delivery, used to allow distinct gel depot formation, is a route of administration for multiple clinical vaccines.[52] We showed that 56 days after administration, the TLR7/8a-NP gels led to 6-fold, 19-fold, and 126-fold higher antibody titers compared to AddaVax, TLR7/8a-Sol gel, and Alum, respectively. Additionally, mice receiving the gel-based vaccine maintained antibody titers above the AddaVax group's peak titer for over 140 days (SI Figure 3). The increased area under the curve (AUC) of the titers over time demonstrates that the TLR7/8a-NP gel vaccine formulation led to more potent and durable antigen-specific humoral immune responses compared to TLR7/8a-Sol gel, AddaVax, and Alum (Figure 4c). We saw that the TLR7/8a-NP gels led to higher anti-HA IgG titers than the TLR7/8a-Sol gel and bolus administration of TLR7/8a-NPs or soluble TLR7/8a (R848) (Figure 4d,c, SI Figure 4). These studies demonstrated that having prolonged codelivery of both the antigen and adjuvant is critical for the benefits we measured. Further characterization of the IgG subclasses 56 days after single administration

https://dx.doi.org/10.1021/acsbiomaterials.0c01496
ACS Biomater. Sci. Eng. 2021, 7, 1889−1899

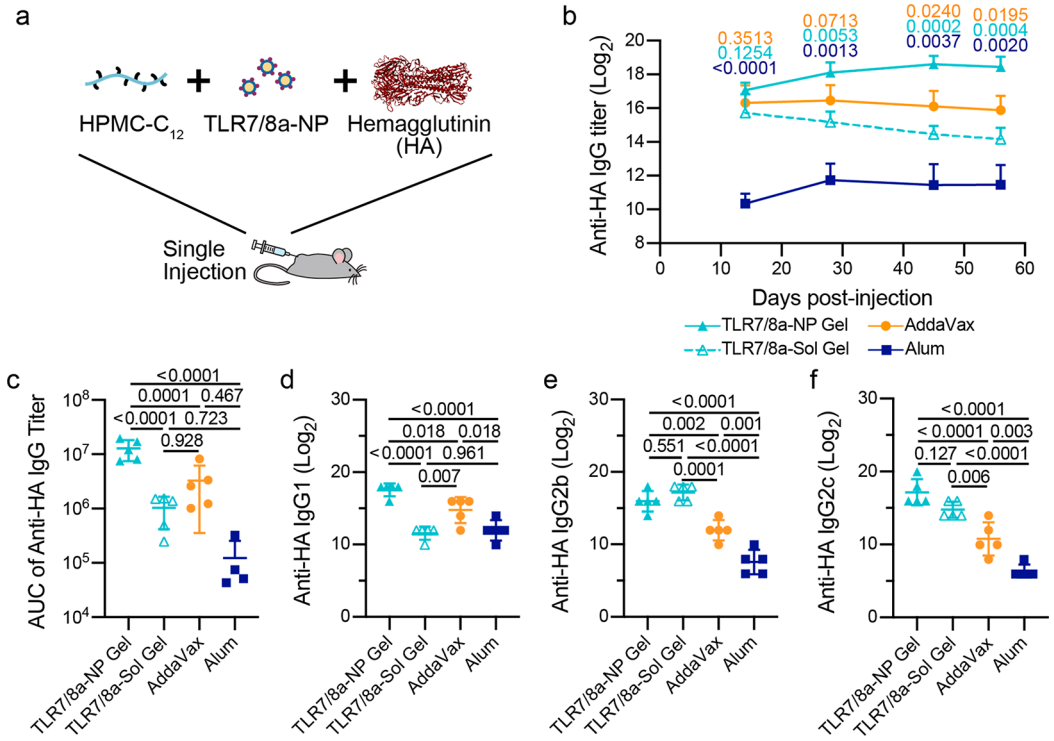

Figure 4. Humoral response to influenza hemagglutinin subunit vaccine. (a) A 2 μg dose of hemagglutinin (HA) was administered subcutaneously in either a PNP gel formulated with 10% TLR7/8a-conjugated nanoparticles (TLR7/8a-NP Gel) and 2% HPMC-C_{12}, 10% unconjugated nanoparticles and soluble TLR7/8a (TLR7/8a-Sol Gel) and 2% HPMC-C_{12}, a bolus of AddaVax (formulated like MF59, the most potent adjuvant used clinically for influenza), or Alum. (b) Serum anti-HA IgG titers from day 14 to day 56 after single injection of HA delivered in TLR7/8a-NP gel, TLR7/8a-Sol gel, an AddaVax bolus, or Alum bolus. P values for TLR7/8a-NP gel compared to Alum (bottom, dark blue), TLR7/8a-Sol gel (middle, light blue), or AddaVax (top, orange) are shown (n = 4 to 5). (c) Area under the curve (AUC) of anti-HA IgG titers (n = 4 to 5) from (b). Serum anti-HA IgG1 (d), IgG2b (e), and IgG2c (f) titers from day 56 after single injection of HA delivered in the TLR7/8a-NP gel, TLR7/8a-Sol gel, AddaVax bolus, or Alum bolus. All error bars are mean ± s.d., P values determined by two-way ANOVA with Tukey's post hoc test (b) or one-way ANOVA with Tukey's post hoc test (c–f).

showed that TLR7/8a-NP gel delivery led to a significant increase in IgG1, IgG2b, and IgG2c antibodies compared to both adjuvant controls (Figure 4d–f). Notably, we saw an 84-fold increase in IgG2c titers for the TLR7/8a-NP gel-based vaccine compared to AddaVax, which is the most important IgG subclass in C57BL/6 mice for fighting viral infections.[53]

To evaluate cross reactivity of serum to HA variants not included in the vaccine formulation, total IgG titers against HA from "future" influenza variants A/California/07/2009(H1N1) (Cal09) and A/Michigan/45/2015(H1N1) (Mich15), as well as A/PuertoRico/8/1934(H1N1) (PR8) (SI Figure 5), were quantified (Figure 5). Serum from animals immunized with A/Brisbane/59/2007(H1N1) (Bris07) HA in TLR7/8a-NP gels exhibited a 16-fold, 64-fold, and 3.4-fold increase in titers against Cal09, Mich15, and PR8 HA variants compared to delivery with AddaVax adjuvant, respectively, and a 256-fold, 64-fold, and 16-fold increase in titers against Cal09, Mich15, and PR8 HA variants compared to delivery with Alum adjuvant, respectively (Figure 5c–e). The breadth can also be visualized by plotting the heterologous titers (Cal09, Mich15, PR8) against the homologous titer (Bris07) (Figure 5f–g). These plots further demonstrate the increase in vaccine potency across multiple "future" HA variants after single administration of Bris07 HA in the TLR7/8a-NP gel. Remarkably the difference in titer between the TLR7/8a-NP gel and the TLR7/8a-Sol gel was much higher with these heterologous HA variants compared to the homologous HA, demonstrating the influence of prolonged codelivery of antigen and adjuvant on improving the breadth of the antibody response. Taken together, these results indicate that prolonged codelivery of HA and a TLR7/8a in our hydrogel platform significantly increases the breadth of the antibody response compared to the most potent clinical adjuvants.

DISCUSSION

The results described in this study provide multiple insights into how to use material strategies to better control the delivery of adjuvants and antigens, specifically TLR7/8 agonists and HA, for improving influenza vaccination. We demonstrate that the conjugation of TLR7/8a to PEG-PLA NPs is able to increase the hydrodynamic diameter of the small molecule, while maintaining its bioactivity. For our application this allowed the TLR7/8a to have slower diffusion in the PNP gel and therefore have matched delivery kinetics to the HA as shown by FRAP experiments. The approach of tethering adjuvants to NPs can be more broadly applied to prolonged delivery hydrogels, as the increase hydrodynamic radius will enable prolonged release across many different materials platforms.

We see that the slow codelivery of TLR7/8a with antigen is critical in achieving improved antibody titers and breadth, as the soluble TLR7/8a (R848) formulation of the vaccine did not match the performance of the TLR7/8a-NP gel. Furthermore, bolus administration of the TLR7/8a-NP on their own with the HA antigen did not lead to improvements in antibody responses. From these results we can conclude that

https://dx.doi.org/10.1021/acsbiomaterials.0c01496
ACS Biomater. Sci. Eng. 2021, 7, 1889–1899

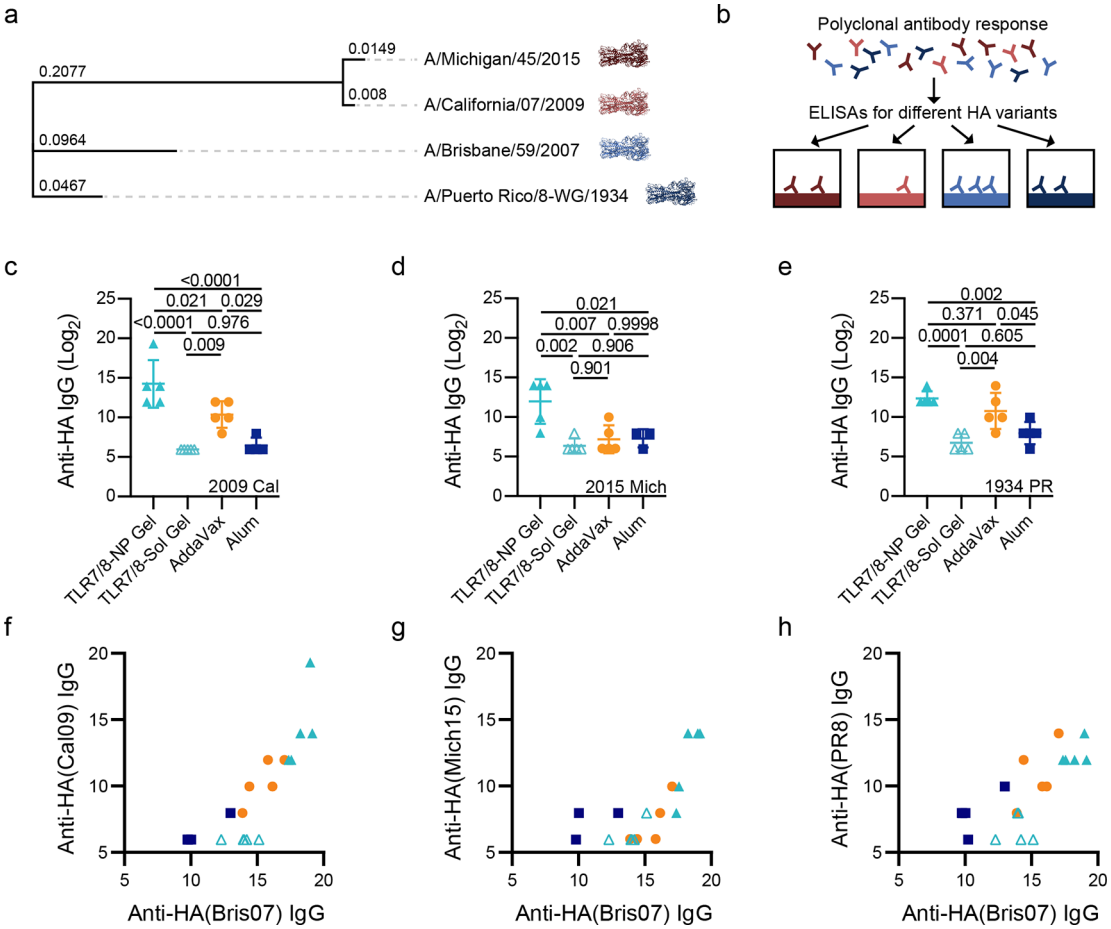

Figure 5. Increased breadth of antibodies toward future influenza strains. (a) Phylogenetic tree of A/Michigan/45/2015(H1N1) (Mich15), A/California/07/2009(H1N1) (Cal09), A/Brisbane/59/2007(H1N1) (Bris07), and A/Puerto Rico/8-WG/1934(H1N1) (PR8) influenza antigens based on HA DNA sequence where the branch lengths represent modifications per site. The tree was created using the 'Generate Phylogenetic Tree' tool on the NIAID Influenza Research Database (IRD) through the Web site at http://www.fludb.org. (b) Experimental schematic showing how ELISAs can be used to measure the breadth of anti-HA responses. Anti-HA titers for Cal09 (c), Mich15 (d), and PR8 (e) for serum from day 56 after single injection of Bris07 HA antigen delivered in the TLR7/8a-NP gel, TLR7/8a-Sol gel, or as a bolus with AddaVax or Alum. Cal09 (f), Mich15 (g), and PR8 (h) titers plotted against Bis07 titers demonstrated that the TLR7/8a-NP gels led to the most potent antibody response across multiple HA variants. All error bars are mean ± s.d., P values determined by one-way ANOVA with a Tukey's post hoc test.

sustained codelivery of both the antigen and adjuvant is beneficial to initiating a broad anti-HA antibody response. We have previously shown that sustained delivery of the OVA and Poly(I:C) model vaccine led to an inflammatory niche and prolonged GCs after a single administration.[19] We expect that the TLR7/8a-NP gel delivering HA has the same effect on the vaccine response, whereby prolonging the exposure to both antigen and adjuvant within the PNP hydrogel creates a local environment where TLR7/8a and HA are able to have extended interactions with innate immune cells due to their similar diffusion release profiles. These cells secrete critical cytokine and chemokines to attract more cells toward the site of injection and enhance antigen processing and presentation. In the GCs, the extended vaccine release allows for prolonged GCs and more cycles of affinity maturation. This guides the immune response toward the creation of higher affinity antibodies and could lead to the increased breadth that we demonstrated.

An important aspect of influenza vaccine development is to find strategies to initiate potent and durable antibody responses against "future" strains of influenza that are not incorporated in the vaccine itself. To compare the impact of slow Bris07-based vaccine delivery in the TLR7/8a-NP gel compared to AddaVax, which is the most potent clinical adjuvant system currently used, we can characterize breadth as a ratio of the titer against a heterologous HA to the titer against the homologous HA (i.e., $\text{titer}_{\text{Cal09 or Mich09}}/\text{titer}_{\text{Bris07}}$). Such an analysis shows that TLR7/8a-NP gels exhibited 2.3-fold and 3.9-fold greater breadth of responses than AddaVax for Cal09 and Mich15, respectively. These observations corroborate previous work evaluating the impact of slow HIV vaccine delivery on the breadth of responses[21] and suggests that prolonged delivery technologies are a powerful tool for achieving more potent, durable, and broad vaccine responses and may play an important role in developing a truly universal flu vaccine.

CONCLUSIONS

In conclusion, sustained delivery of subunit influenza vaccines can be achieved using PNP hydrogels to increase the potency, durability, and breadth of the humoral immune response. We have shown that the PNP hydrogel delivery platform can be adapted through conjugation of small molecule adjuvants to structural motifs within the hydrogels in order to engineer a

https://dx.doi.org/10.1021/acsbiomaterials.0c01496
ACS Biomater. Sci. Eng. 2021, 7, 1889−1899

truly modular sustained delivery system to prolong influenza subunit vaccine exposure. This facile and mild fabrication of these materials by simple mixing can enable robust encapsulation of essentially any antigen, while the precisely controlled delivery characteristics can enable future studies aimed at elucidating the mechanisms by which slow exposure kinetics improve vaccine responses. When paired with sophisticated antigens, the PNP hydrogel delivery system has the potential to form the basis of next-generation vaccines against challenging pathogens such as influenza that continue to pose enormous risks to public health worldwide.

■ ASSOCIATED CONTENT

Supporting Information

The Supporting Information is available free of charge at https://pubs.acs.org/doi/10.1021/acsbiomaterials.0c01496.

TLR7/8 agonist and TLR7/8-agonist−PEG-PLA syntheses, additional anti-HA antibody responses, HA phylogenetic tree, NP characterization, and cargo and polymer diffusivities (PDF)

■ AUTHOR INFORMATION

Corresponding Author

Eric A. Appel − *Department of Bioengineering, Department of Materials Science & Engineering, and ChEM-H Institute, Stanford University, Stanford, California 94305, United States; Institute for Immunity, Transplantation & Infection and Department of Pediatrics - Endocrinology, Stanford University School of Medicine, Stanford, California 94305, United States;* orcid.org/0000-0002-2301-7126; Email: eappel@stanford.edu

Authors

Gillie A. Roth − *Department of Bioengineering, Stanford University, Stanford, California 94305, United States;* orcid.org/0000-0002-3451-3694

Olivia M. Saouaf − *Department of Materials Science & Engineering, Stanford University, Stanford, California 94305, United States*

Anton A. A. Smith − *Department of Materials Science & Engineering, Stanford University, Stanford, California 94305, United States*

Emily C. Gale − *Department of Biochemistry, Stanford University School of Medicine, Stanford, California 94305, United States;* orcid.org/0000-0002-6536-3027

Marcela Alcántara Hernández − *Department of Microbiology & Immunology and Program in Immunology, Stanford University School of Medicine, Stanford, California 94305, United States*

Juliana Idoyaga − *Department of Microbiology & Immunology, Program in Immunology, and Institute for Immunity, Transplantation & Infection, Stanford University School of Medicine, Stanford, California 94305, United States; ChEM-H Institute, Stanford University, Stanford, California 94305, United States*

Complete contact information is available at: https://pubs.acs.org/10.1021/acsbiomaterials.0c01496

Author Contributions

○G.A.R. and O.M.S. contributed equally. The manuscript was written through contributions of all authors. All authors have given approval to the final version of the manuscript.

Notes

The authors declare the following competing financial interest(s): G.A.R., E.C.G., A.A.A.S., and E.A.A. are listed as inventors on patent applications (63/025,845; 62/739,587) describing the technology reported in this manuscript.

■ ACKNOWLEDGMENTS

This research was financially supported by the Center for Human Systems Immunology with Bill & Melinda Gates Foundation (OPP1113682), the Bill & Melinda Gates Foundation (OPP1211043), and the American Cancer Society (RSG-18-133-01). A part of this work was performed at the Stanford Nano Shared Facilities (SNSF), supported by the National Science Foundation under award ECCS-1542152, and in the Idoyaga lab, supported by NIH grant R01CA219994. G.A.R. and O.S. are grateful for support thorough NSF Graduate Research Fellowships. A.A.A.S. is grateful for support from the Novo Nordisk Foundation and the Stanford Bio-X Program (NNF18OC0030896). E.C.G. was funded by the NIH-funded Cell and Molecular Biology Training Program (T32 GM007276).

■ REFERENCES

(1) Short, K. R.; Kedzierska, K.; van de Sandt, C. E. Back to the Future: Lessons Learned From the 1918 Influenza Pandemic. *Front. Cell. Infect. Microbiol.* **2018**, *8*, 343.

(2) Sun, H.; Xiao, Y.; Liu, J.; Wang, D.; Li, F.; Wang, C.; Li, C.; Zhu, J.; Song, J.; Sun, H.; Jiang, Z.; Liu, L.; Zhang, X.; Wei, K.; Hou, D.; Pu, J.; Sun, Y.; Tong, Q.; Bi, Y.; Chang, K. C.; Liu, S.; Gao, G. F.; Liu, J. Prevalent Eurasian avian-like H1N1 swine influenza virus with 2009 pandemic viral genes facilitating human infection. *Proc. Natl. Acad. Sci. U. S. A.* **2020**, *117* (29), 17204−17210.

(3) Swartz, M. A.; Hirosue, S.; Hubbell, J. A. Engineering Approaches to Immunotherapy. *Sci. Transl. Med.* **2012**, *4* (148), DOI: 10.1126/scitranslmed.3003763.

(4) Wen, Y.; Collier, J. H. Supramolecular peptide vaccines: tuning adaptive immunity. *Curr. Opin. Immunol.* **2015**, *35*, 73−79.

(5) Methot, S. P.; Di Noia, J. M. Molecular Mechanisms of Somatic Hypermutation and Class Switch Recombination. *Adv. Immunol.* **2017**, *133*, 37−87.

(6) Klein, F.; Diskin, R.; Scheid, J. F.; Gaebler, C.; Mouquet, H.; Georgiev, I. S.; Pancera, M.; Zhou, T.; Incesu, R. B.; Fu, B. Z.; Gnanapragasam, P. N.; Oliveira, T. Y.; Seaman, M. S.; Kwong, P. D.; Bjorkman, P. J.; Nussenzweig, M. C. Somatic mutations of the immunoglobulin framework are generally required for broad and potent HIV-1 neutralization. *Cell* **2013**, *153* (1), 126−38.

(7) Crotty, S. T Follicular Helper Cell Biology: A Decade of Discovery and Diseases. *Immunity* **2019**, *50* (5), 1132−1148.

(8) Moyer, T. J.; Zmolek, A. C.; Irvine, D. J. Beyond antigens and adjuvants: formulating future vaccines. *J. Clin. Invest.* **2016**, *126* (3), 799−808.

(9) Irvine, D. J.; Aung, A.; Silva, M. Controlling timing and location in vaccines. *Adv. Drug Deliv Rev.* **2020**, DOI: 10.1016/j.addr.2020.06.019.

(10) Crotty, S. T follicular helper cell differentiation, function, and roles in disease. *Immunity* **2014**, *41* (4), 529−42.

(11) Zeng, Q.; Jewell, C. M. Directing toll-like receptor signaling in macrophages to enhance tumor immunotherapy. *Curr. Opin. Biotechnol.* **2019**, *60*, 138−145.

(12) Zhu, Q.; Egelston, C.; Gagnon, S.; Sui, Y. J.; Belyakov, I. M.; Klinman, D. M.; Berzofsky, J. A. Using 3 TLR ligands as a combination adjuvant induces qualitative changes in T cell responses needed for antiviral protection in mice. *J. Clin. Invest.* **2010**, *120* (2), 607−616.

(13) Kasturi, S. P.; Skountzou, I.; Albrecht, R. A.; Koutsonanos, D.; Hua, T.; Nakaya, H. I.; Ravindran, R.; Stewart, S.; Alam, M.; Kwissa, M.; Villinger, F.; Murthy, N.; Steel, J.; Jacob, J.; Hogan, R. J.; Garcia-

Sastre, A.; Compans, R.; Pulendran, B. Programming the magnitude and persistence of antibody responses with innate immunity. *Nature* **2011**, *470* (7335), 543−U136.
(14) Orr, M. T.; Beebe, E. A.; Hudson, T. E.; Moon, J. J.; Fox, C. B.; Reed, S. G.; Coler, R. N. A Dual TLR Agonist Adjuvant Enhances the Immunogenicity and Protective Efficacy of the Tuberculosis Vaccine Antigen ID93. *Plos One* **2014**, *9* (1), DOI: 10.1371/journal.-pone.0083884.
(15) Tibbitt, M. W.; Dahlman, J. E.; Langer, R. Emerging Frontiers in Drug Delivery. *J. Am. Chem. Soc.* **2016**, *138* (3), 704−17.
(16) Li, J.; Mooney, D. J. Designing hydrogels for controlled drug delivery. *Nat. Rev. Mater.* **2016**, *1* (12), DOI: 10.1038/natrevmats.2016.71.
(17) DeMuth, P. C.; Garcia-Beltran, W. F.; Ai-Ling, M. L.; Hammond, P. T.; Irvine, D. J. Composite Dissolving Microneedles for Coordinated Control of Antigen and Adjuvant Delivery Kinetics in Transcutaneous Vaccination. *Adv. Funct. Mater.* **2013**, *23* (2), 161−172.
(18) Irvine, D. J.; Swartz, M. A.; Szeto, G. L. Engineering synthetic vaccines using cues from natural immunity. *Nat. Mater.* **2013**, *12* (11), 978−990.
(19) Tam, H. H.; Melo, M. B.; Kang, M.; Pelet, J. M.; Ruda, V. M.; Foley, M. H.; Hu, J. K.; Kumari, S.; Crampton, J.; Baldeon, A. D.; Sanders, R. W.; Moore, J. P.; Crotty, S.; Langer, R.; Anderson, D. G.; Chakraborty, A. K.; Irvine, D. J. Sustained antigen availability during germinal center initiation enhances antibody responses to vaccination. *Proc. Natl. Acad. Sci. U. S. A.* **2016**, *113* (43), E6639−E6648.
(20) Roth, G. A.; Gale, E. C.; Alcántara-Hernández, M.; Luo, W.; Axpe, E.; Verma, R.; Yin, Q.; Yu, A. C.; Lopez Hernandez, H.; Maikawa, C. L.; Smith, A. A. A.; Davis, M. M.; Pulendran, B.; Idoyaga, J.; Appel, E. A. Injectable Hydrogels for Sustained Codelivery of Subunit Vaccines Enhance Humoral Immunity. *ACS Cent. Sci.* **2020**, DOI: 10.1021/acscentsci.0c00732.
(21) Boopathy, A. V.; Mandal, A.; Kulp, D. W.; Menis, S.; Bennett, N. R.; Watkins, H. C.; Wang, W.; Martin, J. T.; Thai, N. T.; He, Y.; Schief, W. R.; Hammond, P. T.; Irvine, D. J. Enhancing humoral immunity via sustained-release implantable microneedle patch vaccination. *Proc. Natl. Acad. Sci. U. S. A.* **2019**, *116* (33), 16473−16478.
(22) Cirelli, K. M.; Carnathan, D. G.; Nogal, B.; Martin, J. T.; Rodriguez, O. L.; Upadhyay, A. A.; Enemuo, C. A.; Gebru, E. H.; Choe, Y.; Viviano, F.; Nakao, C.; Pauthner, M. G.; Reiss, S.; Cottrell, C. A.; Smith, M. L.; Bastidas, R.; Gibson, W.; Wolabaugh, A. N.; Melo, M. B.; Cossette, B.; Kumar, V.; Patel, N. B.; Tokatlian, T.; Menis, S.; Kulp, D. W.; Burton, D. R.; Murrell, B.; Schief, W. R.; Bosinger, S. E.; Ward, A. B.; Watson, C. T.; Silvestri, G.; Irvine, D. J.; Crotty, S. Slow Delivery Immunization Enhances HIV Neutralizing Antibody and Germinal Center Responses via Modulation of Immunodominance. *Cell* **2019**, *177* (5), 1153−1171 (e28).
(23) Wu, Y.; Norberg, P. K.; Reap, E. A.; Congdon, K. L.; Fries, C. N.; Kelly, S. H.; Sampson, J. H.; Conticello, V. P.; Collier, J. H. A Supramolecular Vaccine Platform Based on alpha-Helical Peptide Nanofibers. *ACS Biomater. Sci. Eng.* **2017**, *3* (12), 3128−3132.
(24) Hudalla, G. A.; Modica, J. A.; Tian, Y. F.; Rudra, J. S.; Chong, A. S.; Sun, T.; Mrksich, M.; Collier, J. H. A self-adjuvanting supramolecular vaccine carrying a folded protein antigen. *Adv. Healthcare Mater.* **2013**, *2* (8), 1114−9.
(25) Chen, N.; Gallovic, M. D.; Tiet, P.; Ting, J. P.; Ainslie, K. M.; Bachelder, E. M. Investigation of tunable acetalated dextran microparticle platform to optimize M2e-based influenza vaccine efficacy. *J. Controlled Release* **2018**, *289*, 114−124.
(26) Lynn, G. M.; Laga, R.; Darrah, P. A.; Ishizuka, A. S.; Balaci, A. J.; Dulcey, A. E.; Pechar, M.; Pola, R.; Gerner, M. Y.; Yamamoto, A.; Buechler, C. R.; Quinn, K. M.; Smelkinson, M. G.; Vanek, O.; Cawood, R.; Hills, T.; Vasalatiy, O.; Kastenmuller, K.; Francica, J. R.; Stutts, L.; Tom, J. K.; Ryu, K. A.; Esser-Kahn, A. P.; Etrych, T.; Fisher, K. D.; Seymour, L. W.; Seder, R. A. In vivo characterization of the physicochemical properties of polymer-linked TLR agonists that enhance vaccine immunogenicity. *Nat. Biotechnol.* **2015**, *33* (11), 1201−10.
(27) Schudel, A.; Francis, D. M.; Thomas, S. N. Material design for lymph node drug delivery. *Nature Reviews Materials* **2019**, *4* (6), 415−428.
(28) Gale, E. C.; Roth, G. A.; Smith, A. A. A.; Alcántara-Hernández, M.; Idoyaga, J.; Appel, E. A. A Nanoparticle Platform for Improved Potency, Stability, and Adjuvanticity of Poly(I:C). *Advanced Therapeutics* **2020**, *3* (1), 1900174.
(29) Smith, A. A. A.; Gale, E. C.; Roth, G. A.; Maikawa, C. L.; Correa, S.; Yu, A. C.; Appel, E. A. Nanoparticles Presenting Potent TLR7/8 Agonists Enhance Anti-PD-L1 Immunotherapy in Cancer Treatment. *Biomacromolecules* **2020**, DOI: 10.1021/acs.bio-mac.0c00812.
(30) Appel, E. A.; Loh, X. J.; Jones, S. T.; Dreiss, C. A.; Scherman, O. A. Sustained release of proteins from high water content supramolecular hydrogels. *Biomaterials* **2012**, *33*, 4646−4652.
(31) Verbeke, C. S.; Mooney, D. J. Injectable, Pore-Forming Hydrogels for In Vivo Enrichment of Immature Dendritic Cells. *Adv. Healthcare Mater.* **2015**, *4* (17), 2677−87.
(32) Guvendiren, M.; Lu, H. D.; Burdick, J. A. Shear-thinning hydrogels for biomedical applications. *Soft Matter* **2012**, *8* (2), 260−272.
(33) Rodell, C. B.; Kaminski, A. L.; Burdick, J. A. Rational Design of Network Properties in Guest-Host Assembled and Shear-Thinning Hyaluronic Acid Hydrogels. *Biomacromolecules* **2013**, *14* (11), 4125−4134.
(34) Steele, A. N.; Paulsen, M. J.; Wang, H.; Stapleton, L. M.; Lucian, H. J.; Eskandari, A.; Hironaka, C. E.; Farry, J. M.; Baker, S. W.; Thakore, A. D.; Jaatinen, K. J.; Tada, Y.; Hollander, M. J.; Williams, K. M.; Seymour, A. J.; Totherow, K. P.; Yu, A. C.; Cochran, J. R.; Appel, E. A.; Woo, Y. J. Multi-phase catheter-injectable hydrogel enables dual-stage protein-engineered cytokine release to mitigate adverse left ventricular remodeling following myocardial infarction in a small animal model and a large animal model. *Cytokine* **2020**, *127*, 154974.
(35) Webber, M. J.; Appel, E. A.; Meijer, E. W.; Langer, R. Supramolecular biomaterials. *Nat. Mater.* **2016**, *15* (1), 13−26.
(36) Appel, E. A.; del Barrio, J.; Loh, X. J.; Scherman, O. A. Supramolecular Polymeric Hydrogels. *Chem. Soc. Rev.* **2012**, *41*, 6195−6214.
(37) Appel, E. A.; Tibbitt, M. W.; Webber, M. J.; Mattix, B. A.; Veiseh, O.; Langer, R. Self-assembled hydrogels utilizing polymer-nanoparticle interactions. *Nat. Commun.* **2015**, *6*, 6295.
(38) Mann, J. L.; Yu, A. C.; Agmon, G.; Appel, E. A. Supramolecular polymeric biomaterials. *Biomater. Sci.* **2018**, *6* (1), 10−37.
(39) Stapleton, L. M.; Steele, A. N.; Wang, H.; Lopez Hernandez, H.; Yu, A. C.; Paulsen, M. J.; Smith, A. A. A.; Roth, G. A.; Thakore, A. D.; Lucian, H. J.; Totherow, K. P.; Baker, S. W.; Tada, Y.; Farry, J. M.; Eskandari, A.; Hironaka, C. E.; Jaatinen, K. J.; Williams, K. M.; Bergamasco, H.; Marschel, C.; Chadwick, B.; Grady, F.; Ma, M.; Appel, E. A.; Woo, Y. J. Use of a supramolecular polymeric hydrogel as an effective post-operative pericardial adhesion barrier. *Nat. Biomed. Eng.* **2019**, *3* (8), 611−620.
(40) Lopez Hernandez, H.; Grosskopf, A. K.; Stapleton, L. M.; Agmon, G.; Appel, E. A. Non-Newtonian Polymer-Nanoparticle Hydrogels Enhance Cell Viability during Injection. *Macromol. Biosci.* **2019**, *19* (1), No. e1800275.
(41) Appel, E. A.; Tibbitt, M. W.; Greer, J. M.; Fenton, O. S.; Kreuels, K.; Anderson, D. G.; Langer, R. Exploiting Electrostatic Interactions in Polymer-Nanoparticle Hydrogels. *ACS Macro Lett.* **2015**, *4* (8), 848−852.
(42) Yu, A. C.; Chen, H.; Chan, D.; Agmon, G.; Stapleton, L. M.; Sevit, A. M.; Tibbitt, M. W.; Acosta, J. D.; Zhang, T.; Franzia, P. W.; Langer, R.; Appel, E. A. Scalable manufacturing of biomimetic moldable hydrogels for industrial applications. *Proc. Natl. Acad. Sci. U. S. A.* **2016**, *113* (50), 14255−14260.
(43) Yu, A. C.; Lopez Hernandez, H.; Kim, A. H.; Stapleton, L. M.; Brand, R. J.; Mellor, E. T.; Bauer, C. P.; McCurdy, G. D.; Wolff, A. J.,

3rd; Chan, D.; Criddle, C. S.; Acosta, J. D.; Appel, E. A. Wildfire prevention through prophylactic treatment of high-risk landscapes using viscoelastic retardant fluids. *Proc. Natl. Acad. Sci. U. S. A.* **2019**, *116* (42), 20820−20827.
(44) Steele, A. N.; Stapleton, L. M.; Farry, J. M.; Lucian, H. J.; Paulsen, M. J.; Eskandari, A.; Hironaka, C. E.; Thakore, A. D.; Wang, H.; Yu, A. C.; Chan, D.; Appel, E. A.; Woo, Y. J. A Biocompatible Therapeutic Catheter-Deliverable Hydrogel for In Situ Tissue Engineering. *Adv. Healthc Mater.* **2019**, *8* (5), No. e1801147.
(45) Appel, E. A.; Forster, R. A.; Rowland, M. J.; Scherman, O. A. The Control of Cargo Release from Physically Crosslinked Hydrogels by Crosslink Dynamics. *Biomaterials* **2014**, *35*, 9897−9903.
(46) Maikawa, C. L.; Sevit, A.; Lin, B.; Wallstrom, R. J.; Mann, J. L.; Yu, A. C.; Waymouth, R. M.; Appel, E. A. Block copolymer composition drives function of self-assembled nanoparticles for delivery of small-molecule cargo. *J. Polym. Sci., Part A: Polym. Chem.* **2019**, *57* (12), 1322−1332.
(47) Axelrod, D.; Koppel, D. E.; Schlessinger, J.; Elson, E.; Webb, W. W. Mobility measurement by analysis of fluorescence photobleaching recovery kinetics. *Biophys. J.* **1976**, *16* (9), 1055−69.
(48) Grosskopf, A. K.; Roth, G. A.; Smith, A. A.; Gale, E. C.; Lopez Hernandez, H.; Appel, E. A. Injectable Supramolecular Polymer-Nanoparticle Hydrogels Enhance Human Mesenchymal Stem Cell Delivery. *Bioeng. Transl. Med.* **2020**, *5* (1), No. e10147.
(49) Fenton, O. S.; Tibbitt, M. W.; Appel, E. A.; Jhunjhunwala, S.; Webber, M. J.; Langer, R. Injectable Polymer-Nanoparticle Hydrogels for Local Immune Cell Recruitment. *Biomacromolecules* **2019**, *20* (12), 4430−4436.
(50) Tregoning, J. S.; Russell, R. F.; Kinnear, E. Adjuvanted influenza vaccines. *Hum. Vaccines Immunother.* **2018**, *14* (3), 550−564.
(51) Feng, H.; Yamashita, M.; da Silva Lopes, T. J.; Watanabe, T.; Kawaoka, Y. Injectable Excipients as Novel Influenza Vaccine Adjuvants. *Front. Microbiol.* **2019**, *10*, 19.
(52) Ezeanolue, E.; Harriman, K.; Hunter, P.; Kroger, A.; Pellegrini, C. General Best Practice Guidelines for Immunization. Best Practices Guidance of the Advisory Committee on Immunization Practices (ACIP). https://www.cdc.gov/vaccines/hcp/acip-recs/general-recs/administration.html.
(53) Martin, R. M.; Brady, J. L.; Lew, A. M. The need for IgG2c specific antiserum when isotyping antibodies from C57BL/6 and NOD mice. *J. Immunol. Methods* **1998**, *212* (2), 187−192.

https://dx.doi.org/10.1021/acsbiomaterials.0c01496
ACS Biomater. Sci. Eng. 2021, 7, 1889−1899